INFECTION AND IMMUNITY, Nov. 2008, p. 4895–4904 Vol. 76, No. 11
0019-9567/08/$08.00+0 doi:10.1128/IAI.00889-08

Bacillus anthracis Edema Toxin Activates Nuclear Glycogen Synthase Kinase 3β▽

Jason L. Larabee,[1] Kevin DeGiusti,[1] James L. Regens,[2] and Jimmy D. Ballard[1]*

Department of Microbiology and Immunology[1] and Department of Occupational and Environmental Health,[2] University of Oklahoma Health Sciences Center, Oklahoma City, Oklahoma 73104

Received 17 July 2008/Returned for modification 16 August 2008/Accepted 25 August 2008

Bacillus anthracis **edema toxin (ET) generates high levels of cyclic AMP and impacts a complex network of signaling pathways in targeted cells. In the current study, we sought to identify kinase signaling pathways modulated by ET to better understand how this toxin alters cell physiology. Using a panel of small-molecule inhibitors of mammalian kinases, we found that inhibitors of glycogen synthase kinase 3 beta (GSK-3β) protected cells from ET-induced changes in the cell cycle. GSK-3β inhibitors prevented declines in cellular levels of cyclin D1 and c-Jun following treatment of macrophages with ET. Strikingly, cell fractionation experiments and confocal immunofluorescence microscopy revealed that ET activates a compartmentalized pool of GSK-3β residing in the nuclei, but not in the cytoplasm, of macrophages. To investigate the outcome of this event, we examined the cellular location and activation state of β-catenin, a critical substrate of GSK-3β, and found that the protein was inactivated within the nucleus following intoxication with ET. To determine if ET could overcome the effects of stimuli that inactivate GSK-3β, we examined the impact of the toxin on the Wnt signaling pathway. The results of these experiments revealed that by targeting GSK-3β residing in the nucleus, ET circumvents the upstream cytoplasmic inactivation of GSK-3β, which occurs following exposure to Wnt-3A. These findings suggest ET arrests the cell cycle by a mechanism involving activation of GSK-3β residing in the nucleus, and by using this novel mechanism of intoxication, ET avoids cellular systems that would otherwise reverse the effects of the toxin.**

Bacillus anthracis edema factor (EF) is a calcium- and calmodulin-dependent adenylate cyclase that generates high levels of cyclic AMP (cAMP) after delivery into the cell by protective antigen (PA) (20). The three-dimensional structure of EF has been resolved, and its catalytic mechanism is well understood (10, 15, 16, 32). Edema toxin (ET), the combination of PA and EF, suppresses immune responses during the development and progression of anthrax disease (3, 26, 36). ET has also been found to sensitize mice to anthrax lethal toxin (12), increase the expression of anthrax toxin receptors in monocytic cells (22), and reduce cell viability (11, 39). Thus, while EF generates a common second messenger, cAMP, the toxin does so in a way that disrupts normal cellular activities.

ET generates supraphysiological levels of cAMP, which is thought to accumulate in the perinuclear region of the cell (7, 20). In the original description of EF as an adenylate cyclase, Leppla found that treatment of CHO K1A cells with ET increased levels of cAMP by approximately 200-fold (20). In a more recent study by Dal Molin et al., EF was shown to be delivered into the cell via a late endosome pathway, and by remaining associated with this compartment, the toxin generates cAMP in the perinuclear region, with decreasing gradients of cAMP radiating to the periphery of the cell (7). These observations support a toxicity model in which ET disrupts cell function by generating high levels of cAMP in the perinuclear region of the cell, yet the signaling network disrupted by this event remains poorly defined.

To date, three signaling pathways have been found to be influenced by cAMP generated in ET-intoxicated cells. The transcription factor cAMP response binding protein (CREB), which is a downstream target of cAMP signaling activated via phosphorylation by protein kinase A (PKA) (31), is activated in macrophages exposed to ET (19, 22, 27). Conversely, using a *Drosophila* model, Guichard and colleagues found that EF activates hedgehog signaling in a PKA-dependent manner (14). The possible impact of ET intoxication on mitogen-activated protein kinases is not fully resolved, as Paccani et al. also reported that ET can inhibit mitogen-activated protein and stress kinase responses in T lymphocytes (26); however, in a separate study, Comer et al. did not detect a similar effect in T lymphocytes isolated from mice treated with ET (5).

There is good reason to suspect that other signaling pathways are part of the network disrupted by ET. Not all of the ET-induced changes in cell physiology can be attributed to activation of CREB, and whether hedgehog signaling plays any role in innate immunity is unclear. Intoxication with ET leads to macrophage death (39) and lymphocytolysis (11), but PKA phosphorylation of CREB promotes cell survival and, in extreme cases, oncogenesis (34). Thus, it is difficult to reconcile all the changes in cell physiology with activation of CREB in ET-intoxicated cells. In line with the idea of CREB-independent effects of ET, Raymond et al. discovered that ET-mediated reduction in phospholipase A2 levels does not involve activation of CREB (28). Kim et al. also found that a portion of transcriptional changes in ET-treated bone marrow-derived macrophages are CREB independent (19). These observations suggest cAMP generated from ET modulates a network of

* Corresponding author. Mailing address: University of Oklahoma Health Sciences Center, BRC-362A, 975 NE 10th Street, Oklahoma City, OK 73104. Phone: (405) 271-3855. Fax: (405) 271-3874. E-mail: jimmy-ballard@ouhsc.edu.

▽ Published ahead of print on 2 September 2008.

signaling events, both CREB dependent and CREB independent, which lead to immunosuppression and cell death.

In the current study, we identify glycogen synthase kinase 3β (GSK-3β) as a protein modulated by cAMP in ET-intoxicated cells and show that inhibition of GSK-3β protects cells from ET-induced cell cycle arrest. The experimental data also indicate that ET activates a nuclear, but not cytoplasmic, pool of GSK-3β, and this leads to inactivation of β-catenin within the nucleus. These findings provide insight into the mechanisms of ET actions and expand our knowledge of the complex signaling network disrupted by this toxin.

MATERIALS AND METHODS

Antibodies, chemical inhibitors, cAMP analogues, and isolation of recombinant proteins. Antibodies recognizing β-catenin (no. 9562); p-S33, p-S37, and p-T41 β-catenin (no. 9561); CREB (no. 9197); GSK-3β (no. 9332); p-S9 GSK-3β (no. 9336); histone 3 (no. 9715); cyclin D1 (no. 2926); or c-Jun (no. 9165) were obtained from Cell Signaling Technology (Beverly, MA). Antibody to p-S9 GSK-3β (sc-11757) for immunofluorescence was obtained from Santa Cruz Biotechnology. The anti-glyceraldehyde 3-phosphate dehydrogenase (GAPDH) mouse monoclonal antibody (ab8245) was acquired from Abcam (Cambridge, MA). LiCl, SB216763, and TDZD-8 were obtained from Sigma Chemical. Lactacystin was obtained from Calbiochem. The following cAMP analogues were obtained from Biolog (Bremen, Germany). N^{6-}-monobutyryladenosine-3′,5′-cyclic monophosphate (6-MB-cAMP) is a membrane-permeable activator of PKA. 8-(4-Chlorophenylthio)-2′-*O*-methyladenosine-3′,5′-cyclic monophosphate (8-CPT-2′-*O*-Me-cAMP) is a membrane-permeable potent activator of *e*xchange *p*rotein directly *a*ctivated by *c*AMP (Epac) and is a poor activator of PKA. PA, EF, and EF K346R were expressed and purified as previously described (39).

Cell culture. RAW 264.7 and L-929 cells were obtained from the American Type Culture Collection (ATCC) (Manassas, VA). The cells were grown in the presence of RPMI 1640 medium (Gibco) supplemented with 10% fetal bovine serum (FBS) (ATCC) and antibiotics or in the presence of Dulbecco's modified Eagle's medium (ATCC) containing 10% fetal bovine serum (ATCC). All cell lines were used between passages 5 and 20.

Wnt-3A conditioned medium and isolation of bone marrow-derived macrophages (BMDM). To produce L-929 cell-conditioned medium, necessary for the growth of primary macrophages, L-929 cells were cultured at a density of 1.25×10^5 cells per ml. On the fifth day of growth, the conditioned medium was removed, passed through a 0.2-μm filter, and stored at −80°C. Also, Wnt-3A conditioned medium was produced from L-929 cells stably transfected with the Wnt-3A gene under the control of the PGK promoter (ATCC CRL-2647). To produce the Wnt-3A conditioned medium, transfected L-929 cells were cultured at a density of 1.25×10^5 per ml in DMEM containing 10% FBS, and the cells were grown for 4 days. At that point, the medium was removed and replaced with fresh medium. The culture grew for an additional 3 days, and the medium was again removed. The media from both the 4- and 3-day incubations were passed through a 0.2-μm filter and stored at 4°C. For use in experiments, the two batches of conditioned medium were combined at a 1:1 ratio, and 5% additional FBS was added. As a control, conditioned medium was similarly generated from the untransfected parental cell line (ATCC CRL-2648).

BMDM from BALB/c mice (handled in accordance with University of Oklahoma IACUC guidelines) were isolated by flushing femurs and culturing the bone marrow cells on bacterial-grade petri dishes in RPMI 1640 medium supplemented with 15% FBS, 30% L-929 cell-conditioned medium, and antibiotics. After 24 h, nonadherent bone marrow cells were removed and cultured for 7 days, at which point the macrophages were subcultured and maintained overnight in RPMI 1640 supplemented with 15% FBS and antibiotics. The cell culture medium was then replaced by fresh medium containing L-929 cell-conditioned medium, and experiments were performed 48 to 72 h later.

Analysis of cell cycle profiles. Cultured macrophages grown in six-well plates were harvested by scraping and then pelleted by centrifugation at $250 \times g$ for 5 min. The cells were resuspended in phosphate-buffered saline (PBS) and fixed overnight at −20°C in 70% ethanol (final concentration). The cells were pelleted at $250 \times g$ for 5 min, washed once with PBS, and resuspended in a PBS solution containing 50 ng/ml propidium iodide, 100 μg/ml RNase A, and 0.01% Triton X-100. The cells were stained for 2 h and then subjected to flow cytometry analysis by using a FACSCalibur system. The resulting cell cycle profiles were evaluated with the Modfit (Verity) and FlowJo data analysis software.

Immunoblot analysis and preparation of total cell extracts. To obtain total cell extracts, cells were grown in six-well plates until approximately 75% confluence was attained. After the cells were subjected to the experimental conditions indicated in each figure legend, they were incubated on ice for 15 min in 400 μl of lysis buffer containing 1% sodium dodecyl sulfate (SDS), 50 mM Tris, pH 7.4, 5 mM EDTA, protease inhibitor cocktail (Sigma catalogue number P8340), and 10 mM *N*-ethylmaleimide. Following incubation on ice, the cells were passed through a 22-gauge needle 10 times and subsequently pelleted via centrifugation at $20{,}000 \times g$ for 5 min to obtain supernatants containing total cellular protein. Protein extracts (10 to 15 μg per well) were mixed with sample buffer (62.5 mM Tris-HCl, pH 6.8, 2% SDS, 10% glycerol, 5% β-mercaptoethanol, and 0.001% bromophenol blue) and heated at 95°C for 10 min, and the proteins were resolved by size using SDS-polyacrylamide gel electrophoresis. The protein bands were transferred to a polyvinylidene difluoride membrane by electroblotting, and the membrane was blocked with 5% nonfat milk in wash buffer (20 mM Tris-HCl, pH 7.5, 100 mM NaCl, and 0.1% Tween 20). The membranes were then probed with primary antibodies and subsequently incubated with the appropriate secondary antibodies conjugated to horseradish peroxidase. The secondary antibody was detected by an enhanced chemiluminescent protein development system (GE Healthcare). Densitometry analysis of immunoblot bands was performed on digitized images using ImageJ 1.37V software (Wayne Rasband, National Institutes of Health). On the digitized images, a box was drawn around each lane, and the pixels were counted, generating lane profile plots. Peaks in the lane profile indicated bands. Using the program tools, the background could be removed and the area under the peaks could be calculated. These area values were then used to determine changes between experimental conditions.

Immunofluorescence staining and confocal microscopy. RAW 264.7 cells were seeded on round coverslips in 12-well plates at 1.5×10^5 cells per ml the night before the experiment. The cells were fixed in 4% paraformaldehyde, washed three times in PBS, and incubated with 100% methanol at −20°C for 10 min. After three additional washes with PBS, the cells were blocked for 2.5 h at 37°C in 1% bovine serum albumin, 5% goat serum, and Tris-buffered saline. The cells were then incubated with the appropriate primary antibody overnight at 4°C and washed three times. Then, goat anti-rabbit immunoglobulin G antibody labeled with Alexa Fluor 568 (Molecular Probes; A11036) was diluted to a concentration of 2 μg/ml in wash buffer and incubated on the cells for 2 h at 37°C. After a series of three washes in wash buffer, the coverslips containing the stained cells were mounted using ProLong Gold antifade reagent with 4′,6′-diamidino-2-phenylindole (DAPI) (Molecular Probes). Confocal images were then taken of the stained cells using a laser scanning confocal microscope (Leica TCS NT), and the images were analyzed using the Leica TCS software.

Subcellular fractionation. Cultured macrophages were grown in T-75 flasks and subjected to experimental conditions. To obtain cells for cytoplasmic and nuclear isolation, the cells were washed, scraped, and then pelleted by centrifugation at $250 \times g$ for 5 min. The cytoplasmic and nuclear fractionations were performed using the NE-PER nuclear and cytoplasmic extraction reagents according to the manufacturer's instructions (Pierce). A protease inhibitor cocktail (Sigma) and 10 mM *N*-ethylmaleimide (Sigma) were added to the extraction reagents. Fractionation was confirmed by examining cytoplasm (GAPDH)- and nucleus (histone 3 and CREB)-specific markers by immunoblotting.

Transfection and luciferase gene reporter assay. Gene reporter plasmids were transfected into RAW 264.7 macrophages using Fugene HD (Roche) following the manufacturer's protocol, which was specific for RAW 264.7 macrophages. After transfection, conditioned medium was added to the cells for approximately 24 h, and the luciferase activity was determined.

Changes in β-catenin/T-cell factor (TCF)-activated gene expression were measured using the Super 8× TOPFlash (Addgene plasmid 12456) and Super 8× FOPFlash (mutant TOPFlash) (Addgene plasmid 12457, originating from the laboratory of R. T. Moon) (38). In some experiments, cells were cotransfected with the pRL-TK vector (Promega), which contains the *Renilla* gene under the control of the constitutive active herpes simplex virus thymidine kinase promoter and which was used to normalize between different experimental sets. The pGL3 vector (Promega) containing the luciferase gene under the control of the simian virus 40 promoter and enhancer sequence was used as a negative control in these experiments. Luciferase was quantified using the Luciferase Assay System (Promega) or the Dual-Luciferase reporter assay system (Promega), followed by measurement of the luminescence signal with a Victor3 (Perkin Elmer) plate reader.

Real-time PCR analysis of *axin2*. cDNA was synthesized from total RNA using SuperScript III (Invitrogen) according the conditions suggested by the manufacturer. For real-time analysis, the resulting cDNA was combined with Power Sybr green PCR master mix (ABI) and primers specific for genes encoding *axin2* or

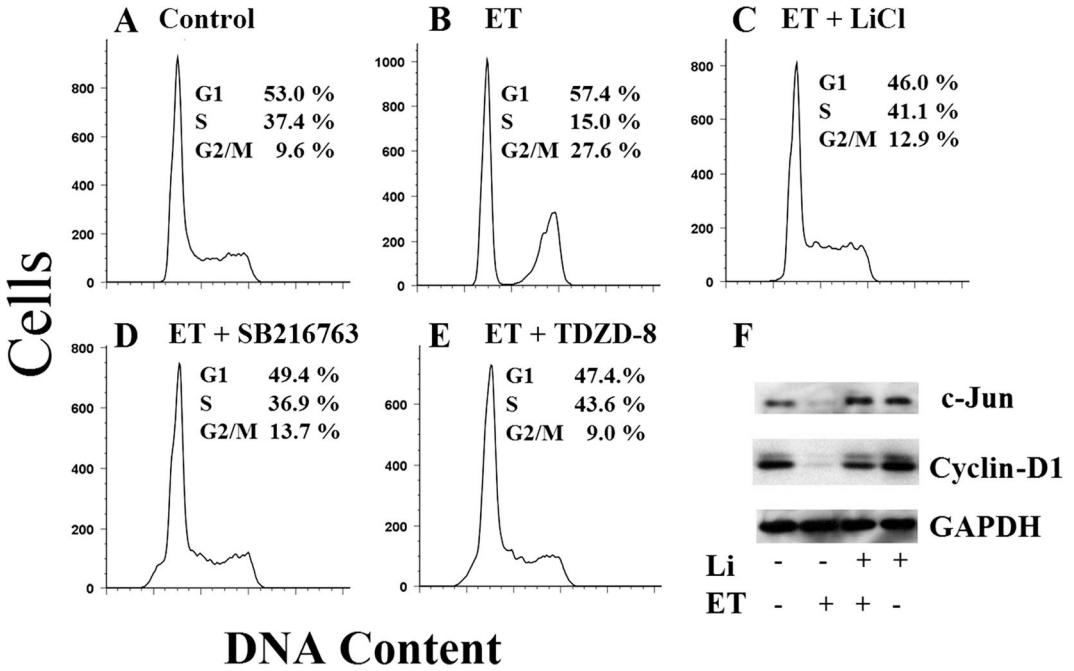

FIG. 1. Impacts of GSK-3β inhibitors on ET-treated macrophages. (A to E) Cells were treated with 10 nM ET (10 nM EF and 10 nM PA) for 6 h, and the cell cycle profiles were determined in the presence or absence of the respective kinase inhibitors (20 mM LiCl, 50 μM SB216763, or 80 μM TDZD-8). (A) Untreated. (B) ET. (C) ET plus LiCl. (D) ET plus SB216763. (E) ET plus TDZD-8. (F) Immunoblot analysis of cyclin D1, c-Jun, and GAPDH from extracts of RAW 264.7 cells treated for 24 h with 10 nM ET in the presence or absence of 20 mM LiCl. The results are representative of at least three experimental repeats.

β-*actin*. Amplification was performed in an Applied Biosystems 7500 Real-Time PCR system, and the comparative cycle at threshold (C_T) method was used to determine relative changes in *axin2* mRNA levels compared to β-*actin* mRNA levels.

Statistics. A two-tailed Student's *t* test (in the statistics module of GraphPad Prism 4) was used to determine *P* values with a 95% confidence interval.

RESULTS

Small-molecule inhibitors of GSK-3β protect cells from ET. ET-sensitive signaling pathways were identified by screening a panel of mammalian kinase inhibitors for the capacity to mimic the effects of the toxin or to protect cells from the effects of the toxin. Because increased levels of cAMP are known to cause cell cycle arrest in cultured macrophages (29), we used changes in the cell cycle profile of ET-intoxicated RAW 264.7 macrophages as a readout in this screen. Kinase inhibitors, such as those targeting mitogen-activated protein kinases, did not protect cells from ET-induced changes in the cell cycle (data not shown). As shown by a comparison between control (Fig. 1A) and ET-treated (Fig. 1B) conditions, cell cycle arrest was observed in macrophages treated with ET for 6 h, and this effect was inhibited by LiCl, SB216763, and TDZD-8 (Fig. 1C to E). Even when incubations were extended to 24 h, LiCl protected against ET-induced cell cycle arrest (data not shown). Finally, treatment with an enzymatically inactive mutant of EF plus PA, PA alone, or EF alone did not alter the cell cycle (data not shown), supporting the idea that the observed changes were dependent on cAMP production by EF. LiCl, SB216763, and TDZD-8 are inhibitors of GSK-3β activity, suggesting the protein was important for mediating the changes in the cell cycle after intoxication by ET in these experiments.

Cyclin D1 and c-Jun modulate the cell cycle and can be regulated by GSK-3β (23, 33). Thus, cultured macrophages were exposed to ET in the presence or absence of LiCl, and cellular levels of cyclin D1 and c-Jun were determined by immunoblotting. As shown in Fig. 1F, cyclin D1 and c-Jun levels were reduced in ET-treated cells, and LiCl prevented this effect. Treatment with an enzymatically inactive mutant of ET did not alter the expression levels of cyclin D1 or c-Jun (data not shown). These results suggested that ET alters the cell cycle in manner that correlates with the loss of cyclin D1 and c-Jun.

ET increases levels of active GSK-3β in the nucleus. A hallmark of GSK-3β activation is decreased phosphorylation at Ser-9 (6), leading us to predict that the cellular levels of GSK-3β phosphorylated at Ser-9 (pS9-GSK-3β) should decrease in ET-treated cells. However, when total cell lysates were probed for changes in the levels of pS9-GSK-3β, the predicted decrease was not observed (Fig. 2A). This observation led us to examine subcellular fractions of GSK-3β to determine if a subpopulation of the kinase modulated the effects of ET. In particular, the fact that GSK-3β can be found in both the nucleus and cytoplasm (2), prompted us to investigate the activation states of the kinase in these two compartments of the cell. The nuclear and cytoplasmic compartments were separated and confirmed by immunoblotting for the cytoplasmic protein GAPDH and for the nuclear protein histone 3. As shown in Fig. 2B and C, the nuclear fraction of untreated macrophages contained high levels of pS9-GSK-3β, but treatment with ET significantly decreased the levels of the phosphorylated form of GSK-3β in the nucleus. In contrast to

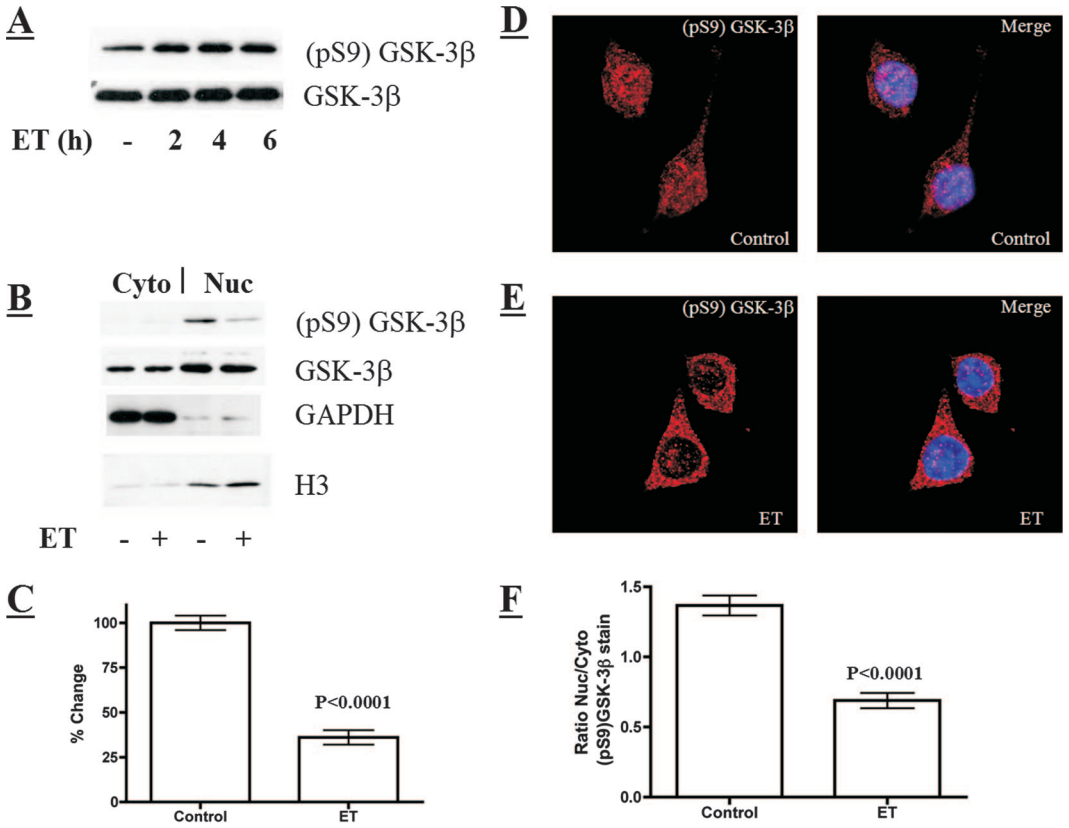

FIG. 2. Analysis of cytoplasmic and nuclear GSK-3β following ET exposure. (A) Immunoblot analysis of phosphorylated-GSK-3β (pS9) and total GSK-3β from total cell lysates of untreated and ET-treated macrophages (10 nM ET). (B) Immunoblot analysis of total and phosphorylated GSK-3β in cytoplasmic (Cyto) and nuclear (Nuc) fractions from control and ET-treated macrophages (6 h of 10 nM ET). (C) Bar graph presenting a densitometry analysis of an immunoblot examining phosphorylated GSK-3β in the nuclei of control and ET-treated macrophages (10 nM ET for 6 h; $n = 9$). (D and E) Phosphorylated GSK-3β examined by indirect immunofluorescence in control and ET-treated macrophages (6 h of 10 nM ET). The confocal microscopy sections show immunofluorescence stain in red (pS9-GSK-3β) and DAPI stain in blue, marking the nucleus. (F) Bar graph showing the ratio of nuclear to cytoplasmic (Nuc/Cyto) phosphorylated GSK-3β in individual cells. These ratios were obtained by performing densitometry on the nuclear and cytoplasmic regions of intact cells analyzed by confocal immunofluorescence microscopy (control, $n = 47$; ET treated, $n = 40$). The error bars indicate the standard errors of the mean, and P values were determined by comparisons between the control and experimental groups using a two-tailed Student's t test with a 95% confidence interval.

changes in the phosphorylation profile, total levels of GSK-3β were not altered in either the cytoplasm or the nucleus when cells were exposed to ET, demonstrating that the toxin does not alter the compartmentalization of the kinase (Fig. 2B). Furthermore, experiments using a nuclear export inhibitor (leptomycin B) did not mimic or alter the effect of ET on pS9-GSK-3β in the nucleus (data not shown). In addition to the subcellular fractionation and immunoblot analyses, confocal immunofluorescence microscopy of intact cells revealed a statistically significant decline in the levels of pS9-GSK-3β in the nuclei of ET-treated macrophages (Fig. 2D and F). Collectively, these findings indicate that exposure to ET increases the level of active GSK-3β residing in the nuclei of cells.

Increased levels of phosphorylated β-catenin in ET-treated macrophages. We next examined the activation state of β-catenin in ET-treated macrophages because the protein is regulated through N-terminal phosphorylation by GSK-3β. We hypothesized that ET-exposed cells would exhibit a decrease in total β-catenin because phosphorylation by GSK-3β targets the protein for ubiquitination and degradation (9). However, as shown in Fig. 3A, immunoblot analysis revealed an increase in overall levels of β-catenin and stabilization of a slower-migrating immunoreactive protein during a 6-h time course of exposure to ET. To determine if the protein that migrated more slowly during SDS-polyacrylamide gel electrophoresis could be a phosphorylated form of β-catenin, an immunoblot was performed on the lysates from ET-treated macrophages using antibody that reacts with three phosphorylated β-catenin residues, pSer-33, pSer-37, and pThr-41, which are known targets of GSK-3β kinase activity (1). Within 6 h of ET intoxication, the levels of phosphorylated β-catenin exhibited a significant increase above that of the control (Fig. 3A and B). Furthermore, phosphorylated β-catenin corresponded in size to the slower-migrating protein detected in the analysis of total β-catenin from ET-treated cells. In contrast, treating cells with an enzymatically inactive form of ET did not alter the phosphorylation state of β-catenin in these cells (Fig. 3C and D). Finally, to confirm that the effects on β-catenin phosphorylation were not unique to the RAW 264.7 macrophage cell line, a similar analysis was performed on primary BMDM. As shown in Fig. 3E and F, treatment of BMDM also triggered an increase in the level of phosphorylated β-catenin. These results

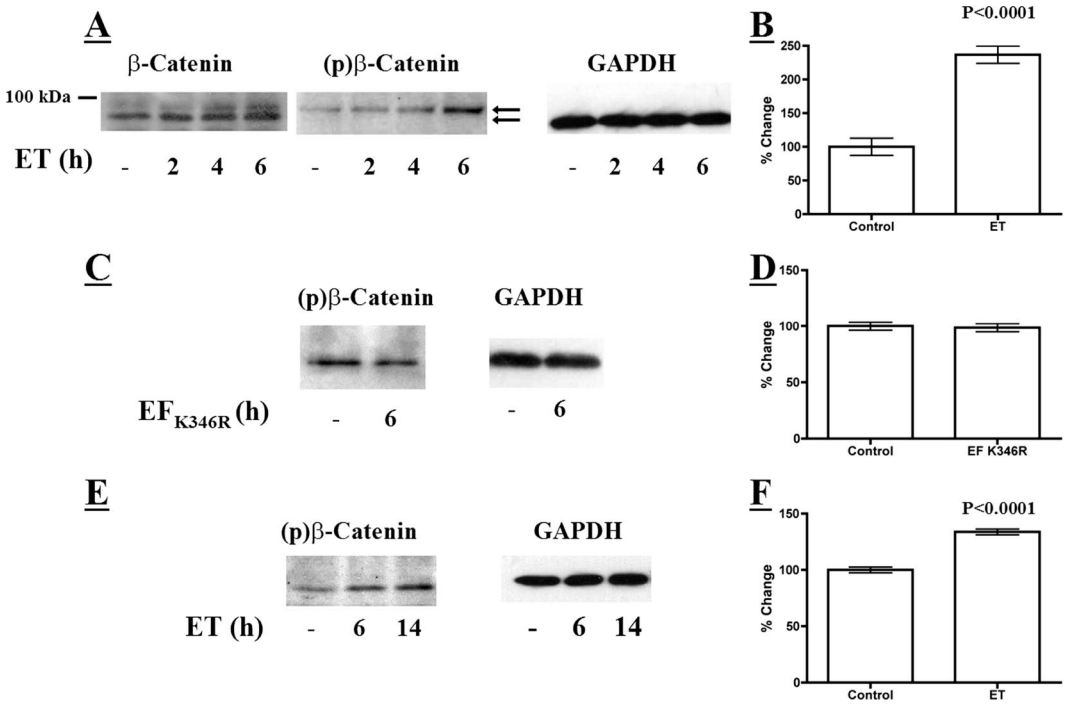

FIG. 3. Levels of phosphorylated β-catenin in cultured macrophages exposed to ET. (A) Immunoblot analysis of total and phosphorylated β-catenin in RAW 264.7 macrophages treated with ET (10 nM EF and 10 nM PA). The upper arrow points to bands indicating phospho-β-catenin. The lower arrow points to unphosphorylated β-catenin. (C) Immunoblot examining levels of phosphorylated β-catenin in RAW 264.7 macrophages treated with enzymatically inactive ET (10 nM EF K346R and 10 nM PA). (E) Immunoblot analyzing phosphorylated β-catenin in mouse BMDM exposed to 10 nM ET. (B, D, and F) Bar graphs displaying densitometry analyses of immunoblots examining phosphorylated β-catenin in ET-treated RAW 264.7 macrophages (B) (10 nM ET for 6 h; $n = 5$), in RAW 264.7 macrophages treated with enzymatically inactive ET (D) ($n = 3$), and in mouse BMDM exposed to ET (F) (10 nM ET for 6 h; $n = 4$). The error bars indicate standard errors of the mean, and the P values were determined by comparisons between the control and experimental groups using a two-tailed Student's t test with a 95% confidence interval.

suggest that ET exposure increases intracellular levels of the phosphorylated form of β-catenin; however, this does not lead to degradation of β-catenin.

PKA agonist activates GSK-3β in the nucleus and increases levels of phosphorylated β-catenin. To determine if nuclear GSK-3β is activated by a PKA-dependent process, we examined GSK-3β after exposing cells to a cell-permeable phosphodiesterase-resistant agonist of PKA (1 mM 6-MB-cAMP). We found that activation of this cAMP-sensitive kinase led to decreased levels of pS9-GSK-3β in the nuclei of macrophages and a corresponding increase in levels of phosphorylated β-catenin (Fig. 4A to D). To determine if activation of GSK-3β might involve other cAMP-activated proteins, we examined the effects of activating Epac, which is a guanosine exchange factor that activates small GTP-binding proteins at the plasma membrane (4). To determine if Epac activation leads to increases in phospho-β-catenin via GSK-3β activation, we treated cells with a cell-permeable phosphodiesterase-resistant agonist of Epac (1 mM 8-CPT-2′-*O*-Me-cAMP). As shown in Fig. 4E, unlike the effects found when cells were treated with the PKA agonist, no discernible changes in the phosphorylation state of β-catenin were detected when cells were treated with the Epac agonist. These observations indicate that PKA activation can mimic the effects of ET on the activation of nuclear GSK-3β.

Phosphorylated β-catenin accumulates in the nuclei of ET-treated macrophages. Because ET increases the level of the active form of GSK-3β in the nucleus, we determined if phosphorylated β-catenin also localized to the nucleus. Nuclear and cytoplasmic fractions were compared by immunoblot analysis, revealing that ET increased levels of phosphorylated β-catenin in the nucleus (Fig. 5A and B). The nuclear compartment integrity was confirmed by immunoblotting for the nuclear protein CREB (Fig. 5A). The nuclear localization of phosphorylated β-catenin was verified by confocal immunofluorescence microscopy with antibodies recognizing phosphorylated β-catenin (Fig. 5C and E). The confocal images revealed colocalization of DAPI-stained DNA and phosphorylated β-catenin and a lack of phosphorylated β-catenin staining in the nucleoli of these cells. In contrast to phosphorylated β-catenin, confocal immunofluorescence microscopy revealed total β-catenin distributed between the cytoplasm and nucleus (Fig. 5D). These results suggested that, like activated GSK-3β, phosphorylated β-catenin is localized to the nuclei of ET-intoxicated cells.

We next examined the impact inhibition of GSK-3β has on nuclear phosphorylated β-catenin in the absence and presence of ET. Inhibition of GSK-3β with LiCl prevented the ET-stimulated increase in the levels of phosphorylated β-catenin within the nucleus (Fig. 6A and B). The ability of LiCl to prevent the phosphorylation of β-catenin also correlates with the ability of LiCl to prevent the ET-induced effects observed in Fig. 1.

Inhibiting the proteasome stabilizes phosphorylated β-catenin in the cytoplasm (30); therefore, proteasome activity was exam-

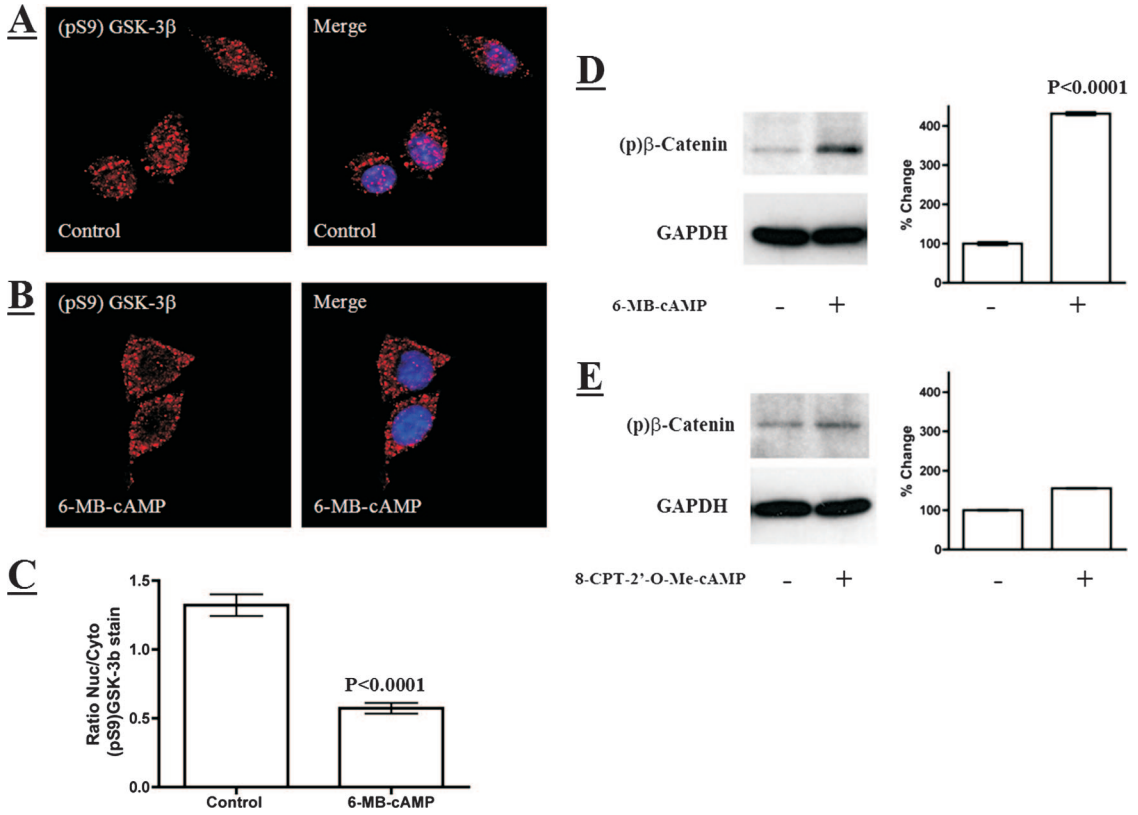

FIG. 4. A PKA activator, 6-MB-cAMP, activates GSK-3β in the nucleus and increases levels of phosphorylated β-catenin. (A and B) Phosphorylated GSK-3β analyzed by indirect immunofluorescence in control and 6-MB-cAMP-treated (1 mM for 5 h) macrophages. The confocal microscopy sections show immunofluorescence stain in red (pS9-GSK-3β) and DAPI stain in blue, marking the nucleus. (C) Bar graph showing the ratio of nuclear to cytoplasmic (Nuc/Cyto) phosphorylated GSK-3β in individual cells. These ratios were obtained by performing densitometry on the nuclear and cytoplasmic regions of intact cells analyzed by confocal immunofluorescence microscopy (control, $n = 40$; 6-MB-cAMP, $n = 34$). (D and E) Immunoblot analysis of phosphorylated β-catenin in RAW 264.7 macrophages after 8-h treatments with 1 mM 6-MB-cAMP (D) or 1 mM 8-CPT-2′-*O*-Me-cAMP (E). 6-MB-cAMP is a specific PKA activator. 8-CPT-2′-*O*-Me-cAMP is a specific activator of Epac and a poor PKA activator. The bar graph associated with each immunoblot displays densitometry analysis of phospho-β-catenin immunoblots ($n = 4$). The error bars indicate standard errors of the mean, and the *P* values were determined by comparisons between the control and experimental groups using a two-tailed Student's *t* test with a 95% confidence interval.

ined as a possible contributor to the observed effects of ET on β-catenin. As expected, treating cultured macrophages with the proteasome inhibitor lactacystin resulted in the accumulation of phosphorylated β-catenin in the cytoplasm above levels observed in control or ET-exposed macrophages (Fig. 6C and D). However, lactacystin treatment did not increase levels of nuclear phosphorylated β-catenin to the degree observed during ET treatment (Fig. 6C and D). This result suggests that proteasome inhibition in the cytoplasm does not account for accumulation of phosphorylated β-catenin in the nucleus.

ET prevents Wnt-3A-mediated activation of β-catenin. Because ET appeared to activate GSK-3β in the nucleus, which is downstream of most cytoplasmic mechanisms of inactivating GSK-3β, we hypothesized that the toxin could reverse the effects of stimuli that promote phosphorylation (i.e., inactivation) of GSK-3β in the cytoplasm. We chose the Wnt signaling pathway as a model to test this hypothesis. Interaction of Wnt-3A with frizzled receptors on the cell surface leads to intracellular signaling involving disheveled-mediated dissociation of GSK-3β from a cytoplasmic multimeric complex in which β-catenin would otherwise be inactivated (8). β-Catenin subsequently accumulates in the cytoplasm and then in the nucleus, where it functions as a cotranscriptional activator. To see if ET could circumvent this event by targeting GSK-3β in the nucleus, we examined the effects of the toxin on macrophages treated with Wnt-3A. As shown in Fig. 7A and B, treatment with exogenous Wnt-3A did not affect the level of phosphorylated β-catenin that accumulated in the nuclei of ET-treated macrophages. However, Wnt-3A did increase total levels of β-catenin in both the cytoplasm and nucleus, confirming that the canonical Wnt signaling pathway was activated under these conditions. To determine if ET can circumvent Wnt signaling, we analyzed the ability of β-catenin to activate TCF-mediated transcription in the presence of Wnt-3A and assessed the impact of the toxin on this process. In this experiment, RAW 264.7 macrophages were transfected with a reporter plasmid (pTOPFlash) containing eight TCF/β-catenin enhancer-binding sites upstream of a luciferase reporter gene. RAW $264.7_{pTOPFlash}$ cells were then treated with ET and examined for changes in luciferase activity, indicative of β-catenin activity. As shown in Fig. 7C, addition of Wnt-3A to these cells raised the level of luciferase activity, indicating that β-catenin transcription is induced by Wnt-3A in these cultured macrophages and corre-

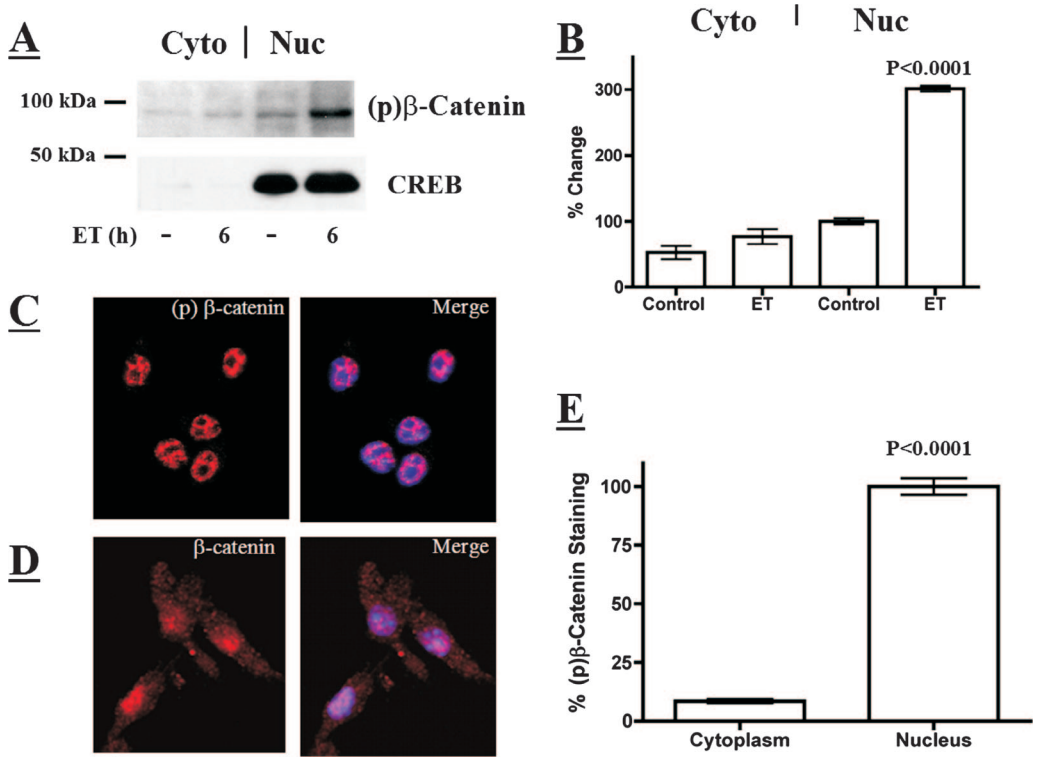

FIG. 5. Detection of phosphorylated β-catenin in the nuclei of RAW 264.7 macrophages. (A) Immunoblot analysis of cytoplasmic and nuclear phospho-β-catenin and CREB in ET-treated RAW 246.7 cells (6 h; 10 nM ET). (B) Bar graph presenting densitometry analysis of an immunoblot examining phosphorylated β-catenin in the nuclear (Nuc) and cytoplasmic (Cyto) fractions from control and ET-treated macrophages (6 h; 10 nM ET; $n = 3$). (C and D) Indirect immunofluorescence of phosphorylated β-catenin and β-catenin in macrophages. The confocal microscopy sections show immunofluorescence stain in red (phospho-β-catenin or β-catenin) and DAPI stain in blue, marking the nucleus. (E) Bar graph showing the percent difference between phospho-β-catenin in the nuclei and cytoplasm of individual cells. These data were obtained by performing densitometry on the nuclear and cytoplasmic regions of intact cells analyzed by confocal immunofluorescence microscopy ($n = 24$). The error bars indicate standard errors of the mean, and the *P* values were determined by comparisons between the control and experimental groups using a two-tailed Student's *t* test with a 95% confidence interval.

lates with the biochemical changes shown in Fig. 7A. However, in line with the results shown in Fig. 7A, treatment with ET reduced the relative luciferase activity in RAW $264.7_{pTOPFlash}$ macrophages exposed to Wnt-3A. When a similar analysis was performed using a plasmid containing a constitutively expressed luciferase gene under the control of a simian virus 40 promoter, intoxication did not result in decreased activity (data not shown). These data suggest that ET reduces the transcriptional activity of TCF/β-catenin in the presence of Wnt-3A. Experiments next examined the expression levels of *axin2*, which is a β-catenin-responsive gene highly induced by Wnt-3A stimulation (17, 21). Using a real-time PCR approach, the levels of *axin2* mRNA were found to increase when macrophages were exposed to exogenous Wnt-3A. However, this *axin2* induction was abrogated when ET was added to the Wnt-3A-exposed cells (Fig. 7D). These findings indicate that activation of nuclear GSK-3β can overcome the effects of upstream cytoplasmic inactivation of the kinase.

DISCUSSION

The findings of the current study support the idea that *B. anthracis* ET activates a nucleus-specific fraction of GSK-3β. Although the phosphorylation state of GSK-3β does not change dramatically in total cell lysates from ET-exposed cells, the nuclear fraction of GSK-3β is markedly reduced in phosphorylation at Ser-9, indicative of activation (Fig. 2). The data also revealed that activation of GSK-3β by ET leads to increased levels of triphosphorylated β-catenin exclusively in the nucleus, which can be reversed by an inhibitor of GSK-3β (Fig. 6A). Finally, these experiments indicate that ET is capable of activating nuclear GSK-3β under standard growth conditions and following induction of the Wnt signaling pathway (Fig. 7). Overall, this study revealed a previously undescribed effect of a bacterial virulence factor and indicates that GSK-3β is part of the network of signaling proteins altered by ET.

GSK-3β is known to phosphorylate at least 40 proteins, 18 of which are transcription factors (e.g., NFAT, c-Myc, c-Jun, and HSF-1) (18). Generally, proteins are inactivated when they become phosphorylated by GSK-3β, suggesting that ET could broadly impact cell physiology by activating GSK-3β. It is also noteworthy that GSK-3β is subject to regulation in the cytoplasm, where it can be dissociated from multimeric complexes and phosphorylated by proteins such as Akt (13). Conversely, GSK-3β in the nucleus may not be subject to these regulatory systems and could be more susceptible to sustained activation. Thus, ET appears to have developed an effective strategy to activate GSK-3β in a cellular compartment that contains many of the substrates for the kinase yet is also excluded from the

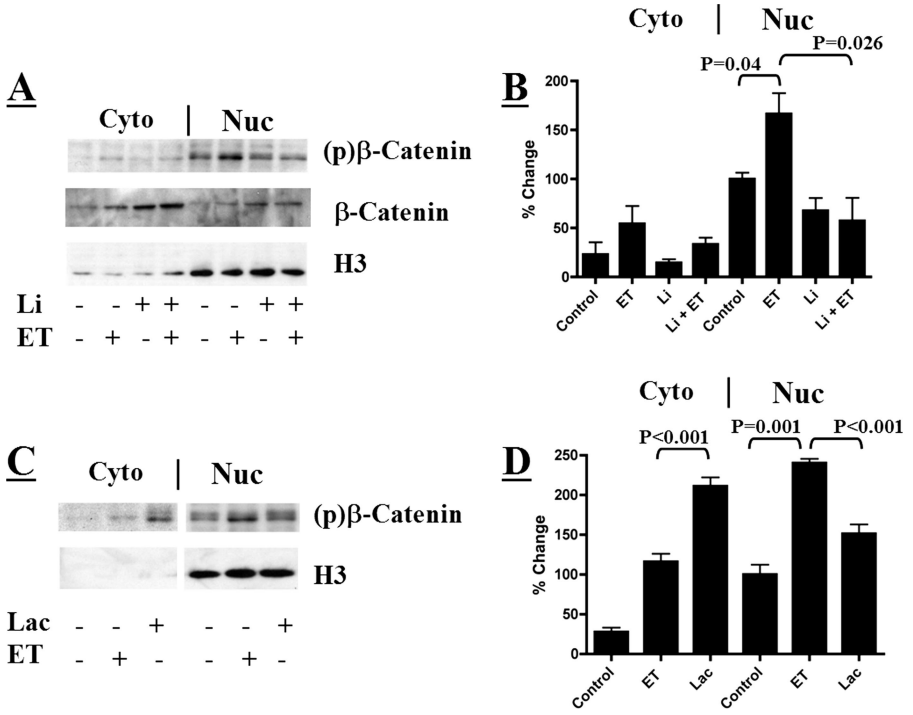

FIG. 6. Effects of a GSK-3β inhibitor and lactacystin on nuclear phospho-β-catenin. (A) Immunoblot analyzing the phosphorylation states of nuclear (Nuc) and cytoplasmic (Cyto) β-catenin in ET-treated RAW 264.7 cells (10 nM for 6 h) in the presence or absence of LiCl (20 mM for 6 h). (C) Immunoblot examining the phosphorylation states of nuclear and cytoplasmic-β-catenin in RAW 264.7 cells treated with 10 nM ET for 6 h or 10 μM lactacystin for 2 h. (B and D) Bar graphs displaying densitometry analysis of immunoblots examining phosphorylated β-catenin in the nuclear and cytoplasmic fractions. (B) Untreated and ET-treated RAW 264.7 macrophages in the presence or absence of LiCl ($n = 3$). (D) RAW 264.7 macrophages treated with 10 nM ET for 6 h or 10 μM lactacystin for 2 h ($n = 4$). The error bars indicate standard errors of the mean, and the *P* values were determined by comparisons between the control and experimental groups using a two-tailed Student's *t* test with a 95% confidence interval.

systems that could reverse the effects of the toxin by inactivating GSK-3β.

As mentioned, GSK-3β targets several substrates. In this study, we selected one of the best defined of these targets, β-catenin, to better understand the effects of ET on this signaling pathway and the outcome of the activation of nuclear GSK-3β. Under basal conditions, GSK-3β phosphorylates β-catenin in the cytoplasm, where it is targeted to the proteasome and degraded (25). In the canonical Wnt signaling pathway, treatment of cells with Wnt-3A promotes the disheveled-mediated dissociation of GSK-3β from a multimeric complex that otherwise supports phosphorylation of β-catenin (37). As a result of stimulation by Wnt-3A, β-catenin accumulates in the cytoplasm and subsequently translocates to the nucleus, where it promotes transcription. Based on this current understanding of the Wnt pathway, it is possible that the intoxication effects of ET could be reversed if the toxin were to target GSK-3β in the cytoplasm. That is, if ET were to target GSK-3β in the cytoplasm, these effects could simply be reversed when cells were exposed to stimuli such as Wnt ligands. However, our data show that by targeting GSK-3β in the nucleus ET is able to overcome Wnt stimulation and reduced β-catenin-dependent transcription by promoting phosphorylation of the cotranscription factor (Fig. 7). Again, this emphasizes that targeting nuclear, but not cytoplasmic, GSK-3β is an effective intoxication strategy for ET.

Previous studies have shown that inhibition of the proteasome increases the levels of phospho-β-catenin, and this phosphorylated form of the protein can accumulate in the nucleus (30). Therefore, we designed experiments that closely examined the possibility that intoxication with ET had a similar effect. Based on the data obtained from these experiments, we believe the effects of ET on β-catenin occur in a manner independent of the proteasome. First, lactacystin treatment prevents the proteasome from degrading phospho-β-catenin in the cytoplasm, allowing the accumulation of that form in the cytoplasm (Fig. 6). ET treatment does not trigger such an increase of phospho-β-catenin in the cytoplasm (Fig. 6), and inhibiting the proteasome with lactacystin did not result in the accumulation of phospho-β-catenin in the nucleus to the level observed when cells were treated with ET (Fig. 6). Second, elevating β-catenin levels through Wnt stimulation does not affect the ability of ET to increase the amount of phospho-β-catenin in the nucleus (Fig. 7A and B). Besides demonstrating that phospho-β-catenin accumulates independently of total β-catenin levels, these experiments provided additional evidence that GSK-3β modifies β-catenin directly in the nuclear compartment, allowing ET to short circuit this signaling pathway.

The results of this study suggest that, similar to reports on cytoplasmic GSK-3β, the phosphorylation state of nuclear GSK-3β contributes to the modulation and inactivation of β-catenin. Indeed, there is a strong correlation in our data

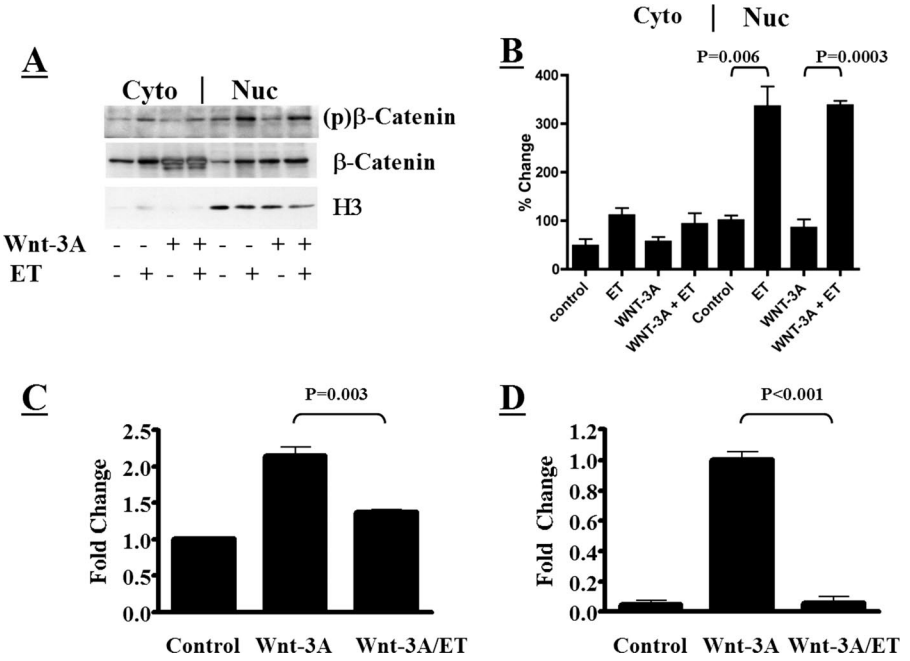

FIG. 7. Changes in β-catenin activity in macrophages exposed to ET in the presence of Wnt-3A. (A) Immunoblot examining the phosphorylation states of nuclear (Nuc) and cytoplasmic (Cyto) β-catenin in ET-treated RAW 264.7 cells (10 nM; 6 h) following activation of the canonical Wnt signaling pathway with Wnt-3A (conditioned medium for 24 h). (B) Bar graph showing densitometry analysis of immunoblots examining phosphorylated β-catenin in the nuclear and cytoplasmic fractions from panel A ($n = 3$). (C) Impact of ET (10 nM ET; 6 h) on β-catenin-mediated activation of TCF-regulated transcription in RAW $264.7_{pTOPFLash}$ macrophages with and without Wnt-3A stimulation (conditioned medium for 24 h). (C) Real-time PCR analysis of *axin2* in the presence of Wnt-3A (conditioned medium; 24 h) and ET (10 nM; 6 h). Relative changes in *axin2* expression were compared to β-*actin* expression using the comparative cycle at threshold (C_T) method. The error bars indicate standard errors of the mean, and *P* values were determined by comparisons between the control and experimental groups using a two-tailed Student's *t* test with a 95% confidence interval.

between ET-induced dephosphorylation of nuclear GSK-3β, increased phosphorylation of β-catenin, and reduced β-catenin cotranscriptional activity in cultured macrophages. However, unlike the parallel events observed in the cytoplasm, phosphorylated β-catenin appears to accumulate in the nucleus in this inactive state and is not degraded. Interestingly, the work of Staal et al. found that the level of N-terminal phosphorylation of β-catenin controls the cotranscriptional activity of this protein (35); therefore, even in the absence of degradation, phosphorylated β-catenin is unable to stimulate transcription. Thus, a critical conclusion of these studies is that the well-described biochemical mechanisms supporting the activation of GSK-3β and a corresponding phosphorylation of β-catenin in the cytoplasm also appear to function in the nuclei of macrophages.

In these studies, the activation of PKA by cAMP led to decreased levels of phosphorylated GSK-3β in the nuclei of macrophages, which contrasts with the idea that PKA phosphorylates GSK-3β at the Ser-9 inhibitory site. This suggests that additional steps and proteins may be involved in ET-mediated activation of nuclear GSK-3β, functioning between PKA activation and the reduction in the levels of phosphorylated GSK-3β. Interestingly, a recent study also found that cAMP activates GSK-3β in Reh cells (24). Therefore, PKA-related activation of GSK-3β is not unprecedented; however, in the case of ET-intoxicated cells, this event appears to be restricted to the nucleus.

Overall, these findings provide new insight into a previously undescribed mechanism of action for a well-known bacterial toxin. It will be interesting to learn how the activation of nuclear GSK-3β synergizes with other known ET effects in order to begin to understand the overall mechanism of action for this bacterial toxin.

ACKNOWLEDGMENTS

This research was supported by the Defense Threat Reduction Agency and the Air Force Research Laboratory FA8650-05-2-6523.

REFERENCES

1. **Aberle, H., A. Bauer, J. Stappert, A. Kispert, and R. Kemler.** 1997. Beta-catenin is a target for the ubiquitin-proteasome pathway. EMBO J. **16:**3797–3804.
2. **Bijur, G. N., and R. S. Jope.** 2001. Proapoptotic stimuli induce nuclear accumulation of glycogen synthase kinase-3 beta. J. Biol. Chem. **276:**37436–37442.
3. **Brittingham, K. C., G. Ruthel, R. G. Panchal, C. L. Fuller, W. J. Ribot, T. A. Hoover, H. A. Young, A. O. Anderson, and S. Bavari.** 2005. Dendritic cells endocytose *Bacillus anthracis* spores: implications for anthrax pathogenesis. J. Immunol. **174:**5545–5552.
4. **Cheng, X., Z. Ji, T. Tsalkova, and F. Mei.** 2008. Epac and PKA: a tale of two intracellular cAMP receptors. Acta Biochim. Biophys. Sin. **40:**651–662.
5. **Comer, J. E., A. K. Chopra, J. W. Peterson, and R. Konig.** 2005. Direct inhibition of T-lymphocyte activation by anthrax toxins in vivo. Infect. Immun. **73:**8275–8281.
6. **Cross, D. A., D. R. Alessi, P. Cohen, M. Andjelkovich, and B. A. Hemmings.** 1995. Inhibition of glycogen synthase kinase-3 by insulin mediated by protein kinase B. Nature **378:**785–789.
7. **Dal Molin, F., F. Tonello, D. Ladant, I. Zornetta, I. Zamparo, G. Di Benedetto, M. Zaccolo, and C. Montecucco.** 2006. Cell entry and cAMP imaging of anthrax edema toxin. EMBO J. **25:**5405–5413.

8. **Ding, V. W., R. H. Chen, and F. McCormick.** 2000. Differential regulation of glycogen synthase kinase 3β by insulin and Wnt signaling. J. Biol. Chem. **275:**32475–32481.
9. **Doble, B. W., and J. R. Woodgett.** 2003. GSK-3: tricks of the trade for a multi-tasking kinase. J. Cell Sci. **116:**1175–1186.
10. **Drum, C. L., S. Z. Yan, J. Bard, Y. Q. Shen, D. Lu, S. Soelaiman, Z. Grabarek, A. Bohm, and W. J. Tang.** 2002. Structural basis for the activation of anthrax adenylyl cyclase exotoxin by calmodulin. Nature **415:**396–402.
11. **Firoved, A. M., G. F. Miller, M. Moayeri, R. Kakkar, Y. Shen, J. F. Wiggins, E. M. McNally, W. J. Tang, and S. H. Leppla.** 2005. *Bacillus anthracis* edema toxin causes extensive tissue lesions and rapid lethality in mice. Am. J. Pathol. **167:**1309–1320.
12. **Firoved, A. M., M. Moayeri, J. F. Wiggins, Y. Shen, W. J. Tang, and S. H. Leppla.** 2007. Anthrax edema toxin sensitizes DBA/2J mice to lethal toxin. Infect. Immun. **75:**2120–2125.
13. **Fukumoto, S., C. M. Hsieh, K. Maemura, M. D. Layne, S. F. Yet, K. H. Lee, T. Matsui, A. Rosenzweig, W. G. Taylor, J. S. Rubin, M. A. Perrella, and M. E. Lee.** 2001. Akt participation in the Wnt signaling pathway through Dishevelled. J. Biol. Chem. **276:**17479–17483.
14. **Guichard, A., J. M. Park, B. Cruz-Moreno, M. Karin, and E. Bier.** 2006. Anthrax lethal factor and edema factor act on conserved targets in *Drosophila*. Proc. Natl. Acad. Sci. USA **103:**3244–3249.
15. **Guo, Q., Y. Shen, Y. S. Lee, C. S. Gibbs, M. Mrksich, and W. J. Tang.** 2005. Structural basis for the interaction of *Bordetella pertussis* adenylyl cyclase toxin with calmodulin. EMBO J. **24:**3190–3201.
16. **Guo, Q., Y. Shen, N. L. Zhukovskaya, J. Florian, and W. J. Tang.** 2004. Structural and kinetic analyses of the interaction of anthrax adenylyl cyclase toxin with reaction products cAMP and pyrophosphate. J. Biol. Chem. **279:** 29427–29435.
17. **Jho, E. H., T. Zhang, C. Domon, C. K. Joo, J. N. Freund, and F. Costantini.** 2002. Wnt/beta-catenin/Tcf signaling induces the transcription of Axin2, a negative regulator of the signaling pathway. Mol. Cell. Biol. **22:**1172–1183.
18. **Jope, R. S., and G. V. Johnson.** 2004. The glamour and gloom of glycogen synthase kinase-3. Trends Biochem. Sci. **29:**95–102.
19. **Kim, C., S. Wilcox-Adelman, Y. Sano, W. J. Tang, R. J. Collier, and J. M. Park.** 2008. Antiinflammatory cAMP signaling and cell migration genes co-opted by the anthrax bacillus. Proc. Natl. Acad. Sci. USA **105:**6150–6155.
20. **Leppla, S. H.** 1982. Anthrax toxin edema factor: a bacterial adenylate cyclase that increases cyclic AMP concentrations of eukaryotic cells. Proc. Natl. Acad. Sci. USA **79:**3162–3166.
21. **Lustig, B., B. Jerchow, M. Sachs, S. Weiler, T. Pietsch, U. Karsten, M. van de Wetering, H. Clevers, P. M. Schlag, W. Birchmeier, and J. Behrens.** 2002. Negative feedback loop of Wnt signaling through upregulation of conductin/axin2 in colorectal and liver tumors. Mol. Cell. Biol. **22:**1184–1193.
22. **Maldonado-Arocho, F. J., J. A. Fulcher, B. Lee, and K. A. Bradley.** 2006. Anthrax oedema toxin induces anthrax toxin receptor expression in monocyte-derived cells. Mol. Microbiol. **61:**324–337.
23. **Mann, B., M. Gelos, A. Siedow, M. L. Hanski, A. Gratchev, M. Ilyas, W. F. Bodmer, M. P. Moyer, E. O. Riecken, H. J. Buhr, and C. Hanski.** 1999. Target genes of beta-catenin-T cell-factor/lymphoid-enhancer-factor signaling in human colorectal carcinomas. Proc. Natl. Acad. Sci. USA **96:**1603–1608.
24. **Naderi, S., K. B. Gutzkow, H. U. Lahne, S. Lefdal, W. J. Ryves, A. J. Harwood, and H. K. Blomhoff.** 2004. cAMP-induced degradation of cyclin D3 through association with GSK-3β. J. Cell Sci. **117:**3769–3783.
25. **Nelson, W. J., and R. Nusse.** 2004. Convergence of Wnt, beta-catenin, and cadherin pathways. Science **303:**1483–1487.
26. **Paccani, S. R., F. Tonello, R. Ghittoni, M. Natale, L. Muraro, M. M. D'Elios, W. J. Tang, C. Montecucco, and C. T. Baldari.** 2005. Anthrax toxins suppress T lymphocyte activation by disrupting antigen receptor signaling. J. Exp. Med. **201:**325–331.
27. **Park, J. M., F. R. Greten, A. Wong, R. J. Westrick, J. S. Arthur, K. Otsu, A. Hoffmann, M. Montminy, and M. Karin.** 2005. Signaling pathways and genes that inhibit pathogen-induced macrophage apoptosis–CREB and NF-kappaB as key regulators. Immunity **23:**319–329.
28. **Raymond, B., D. Leduc, L. Ravaux, R. Le Goffic, T. Candela, M. Raymond-jean, P. L. Goossens, and L. Touqui.** 2007. Edema toxin impairs anthracidal phospholipase A2 expression by alveolar macrophages. PLoS Pathog. **3:**e187.
29. **Rock, C. O., J. L. Cleveland, and S. Jackowski.** 1992. Macrophage growth arrest by cyclic AMP defines a distinct checkpoint in the mid-G1 stage of the cell cycle and overrides constitutive c-myc expression. Mol. Cell. Biol. **12:** 2351–2358.
30. **Sadot, E., M. Conacci-Sorrell, J. Zhurinsky, D. Shnizer, Z. Lando, D. Zharhary, Z. Kam, A. Ben-Ze'ev, and B. Geiger.** 2002. Regulation of S33/S37 phosphorylated beta-catenin in normal and transformed cells. J. Cell Sci. **115:**2771–2780.
31. **Sands, W. A., and T. M. Palmer.** 2008. Regulating gene transcription in response to cyclic AMP elevation. Cell Signal. **20:**460–466.
32. **Shen, Y., N. L. Zhukovskaya, Q. Guo, J. Florian, and W. J. Tang.** 2005. Calcium-independent calmodulin binding and two-metal-ion catalytic mechanism of anthrax edema factor. EMBO J. **24:**929–941.
33. **Shtutman, M., J. Zhurinsky, I. Simcha, C. Albanese, M. D'Amico, R. Pestell, and A. Ben-Ze'ev.** 1999. The cyclin D1 gene is a target of the beta-catenin/LEF-1 pathway. Proc. Natl. Acad. Sci. USA **96:**5522–5527.
34. **Siu, Y. T., and D. Y. Jin.** 2007. CREB—a real culprit in oncogenesis. FEBS J. **274:**3224–3232.
35. **Staal, F. J., M. M. Noort, G. J. Strous, and H. C. Clevers.** 2002. Wnt signals are transmitted through N-terminally dephosphorylated beta-catenin. EMBO Rep. **3:**63–68.
36. **Tessier, J., C. Green, D. Padgett, W. Zhao, L. Schwartz, M. Hughes, and E. Hewlett.** 2007. Contributions of histamine, prostanoids, and neurokinins to edema elicited by edema toxin from *Bacillus anthracis*. Infect. Immun. **75:** 1895–1903.
37. **Thiele, A., M. Wasner, C. Muller, K. Engeland, and S. Hauschildt.** 2001. Regulation and possible function of beta-catenin in human monocytes. J. Immunol. **167:**6786–6793.
38. **Veeman, M. T., D. C. Slusarski, A. Kaykas, S. H. Louie, and R. T. Moon.** 2003. Zebrafish prickle, a modulator of noncanonical Wnt/Fz signaling, regulates gastrulation movements. Curr. Biol. **13:**680–685.
39. **Voth, D. E., E. E. Hamm, L. G. Nguyen, A. E. Tucker, I. I. Salles, W. Ortiz-Leduc, and J. D. Ballard.** 2005. *Bacillus anthracis* oedema toxin as a cause of tissue necrosis and cell type-specific cytotoxicity. Cell Microbiol. **7:**1139–1149.

Editor: J. B. Bliska